Earth and Planetary Science Letters 303 (2011) 240–250

Contents lists available at ScienceDirect

Earth and Planetary Science Letters

journal homepage: www.elsevier.com/locate/epsl

The effect of sediment recycling in subduction zones on the Hf isotope character of new arc crust, Banda arc, Indonesia

O. Nebel [a,b,*], P.Z. Vroon [a], W. van Westrenen [a], T. Iizuka [b], G.R. Davies [a]

[a] Faculty of Earth and Life Sciences, VU University Amsterdam, The Netherlands
[b] Research School of Earth Science, The Australian National University, Canberra, Australia

ARTICLE INFO

Article history:
Received 27 July 2010
Received in revised form 28 December 2010
Accepted 28 December 2010
Available online 5 February 2011

Editor: T.M. Harrison

Keywords:
zircon
Hf–O isotopes
Banda arc
Hadaean subduction

ABSTRACT

A large portion of Earth's crust is formed at convergent plate boundaries that are accompanied by the subduction of sediments that can contain evolved crust-derived detritus. Partial melting of such sediments can strongly affect the trace element and isotope geochemistry of new arc rocks. Here, we present high-precision Lu–Hf–Zr concentration data and Hf isotope compositions for a series of volcanic rocks from the Banda arc, East Indonesia, to quantify the transfer of subducted Hf to the Banda arc crust and address the influence of recycled Hf in subduction zones on the Hf isotope systematics of arc rocks.

Along-arc from NE to SW, the $^{176}Hf/^{177}Hf$ decreases from 0.28314 to 0.28268 ranging from predominantly mantle-like ratios towards more crustal signatures. Hf–Nd isotope co-variations require low Nd/Hf in the arc magma source, inconsistent with fluid addition to the arc melts, but in agreement with the involvement of partial sediment melts. The systematic decrease in Hf–Nd isotopes infers a NE–SW along-arc increase in the involvement of subducted continental material (SCM) in the arc magma source, consistent with $\delta^{18}O$ and Nd–Sr–Pb isotope constraints. The along-arc decrease in Hf isotopes coupled with increasing Zr/Hf (from 31.9 to 36.1) and decreasing Lu/Hf suggests that the newly produced arc lavas contain crustal-derived Hf as a result of partial melting of SCM associated with the breakdown of zircon. Based on recent experimental estimates of temperatures required to achieve zircon breakdown, we infer that slab surface temperatures in the Banda arc region need to be as high as 925 °C.

As a consequence of the inheritance of non-radiogenic Hf from SCM, the juvenile Banda arc crust exhibits Hf isotope model ages biased by hundreds of millions of years. We conclude that crust-formation ages derived from Hf isotope ratios of convergent margin rocks and their constituent minerals (such as zircon) can be geologically meaningless mixing ages, even when they readily preserve low $\delta^{18}O$ values (i.e., <6.5). These findings are discussed with respect to the inferred origin of Hadaean zircons at convergent plate boundaries, which appear consistent with an origin in a convergent margin setting.

© 2011 Elsevier B.V. Open access under the Elsevier OA license.

1. Introduction

The continental crust and the depleted mantle have complementary $^{176}Hf/^{177}Hf$ isotope ratios relative to an evolving chondritic uniform reservoir (CHUR, e.g., Bouvier et al., 2008; Patchett et al., 1981, 2004; Vervoort and Blichert-Toft, 1999). The non-radiogenic Hf isotope character of the continental crust is caused by differences in compatibility of the parent and daughter elements Lu and Hf during partial melting of mantle material, leading to a relative enrichment of Hf over Lu by a factor of 5 relative to the mantle in the incompatible element-enriched crust (Rudnick and Gao, 2003; Salters and Stracke, 2004).

Exchange between the continental crust and the depleted mantle takes place at subduction zones. The (re-)flux of sediments in subduction zones into a depleted mantle reservoir has previously been suggested to be of major importance for the Hf isotope evolution of the mantle (e.g., Chauvel et al., 2008, 2009; Patchett et al., 1981; Pearce et al., 1999; Salters and Hart, 1991; Salters and White, 1996; Vervoort and Blichert-Toft, 1999; Vervoort et al., 1999; White and Patchett, 1984). The introduction of crustal Hf to the mantle has been suggested to cause mantle isotope heterogeneity as observed for example, in ocean island basalts (e.g., Chauvel et al., 2009; Nowell et al., 1998; Salters and Hart, 1991; Vervoort and Blichert-Toft, 1999), or in arc and mid-ocean-ridge rocks in the Indian Ocean (e.g., Kempton et al., 2002; Nebel et al., 2007; Pearce et al., 1999, 2007). Recent estimates suggest ~85% of sediment-derived Hf originating from subducting volcano-clastic debris is transported back to the mantle (Chauvel et al., 2009). The remaining 15% that is transported back to the arc crust through the mantle wedge probably has only minor effects on Hf isotope compositions of newly formed island arc rocks, as its isotope composition is similar to the ambient mantle wedge where arc magmas are generated.

* Corresponding author.
E-mail address: oliver.nebel@anu.edu.au (O. Nebel).

0012-821X © 2011 Elsevier B.V. Open access under the Elsevier OA license.
doi:10.1016/j.epsl.2010.12.053

For sediments in subduction zones that were derived from weathering of more felsic crustal rocks, Hf mobility is controlled by partial melting, as it is considered immobile in hydrous fluids (e.g., Brenan et al., 1995; Class et al., 1999). Although previous field-based studies have pointed out that partial mobility of Hf in slab-derived fluids is possible (Turner et al., 2009; Woodhead et al., 2001), it was concluded that the amount of Hf transported in such fluids is relatively small. As a result, the involvement of sediment-derived melts is generally considered of dominant importance for the Hf budget of arc rocks (e.g., Barry et al., 2006; Marini et al., 2005; Todd et al., 2010; Tollstrup and Gill, 2005; Tollstrup et al., 2010; Yogodzinski et al., 2010). For many elements and isotopic systems, larger contributions of continental sediments result in more crust-like radiogenic isotope ratios in arc rocks. However, in the case of Hf, its transfer is controlled by the behaviour of zircon and garnet during partial melting of sediments (e.g., Carpentier et al., 2009) indicating that the effect of sedimentary recycling is a complex process.

Here, we provide constraints on the effects of subducting zircon as well as residual garnet on the Hf isotope systematics in arc crust by combining Hf–Nd–O isotopic data with trace element geochemistry. Using high-precision isotope dilution techniques, we studied the Lu–Hf–Zr elemental and Hf isotope characteristics of a series of volcanic rocks along the Banda arc, East Indonesia, for which sediment partial melting was suggested to be important on the basis of O–Sr–Nd–Pb isotope studies (e.g., Vroon et al., 1993, 2001). Previous work has shown that our samples exhibit systematic variations in geochemical tracers along the arc front from NE to SW that are linked to progressively increased amounts of subducted continental material (SCM) in their source. The Banda arc thus represents an ideal natural laboratory to systematically study the mobility of Hf in SCM and its effects on Hf isotope ratios in newly formed arc crust; a circumstance that is rarely met by other intra-oceanic arcs or convergent continental margins.

2. Tectonic background and sample selection

At the Banda arc (Fig. 1), the Indian–Australian plate is subducting NNE-wards underneath the Southeast-Asian Plate, and is

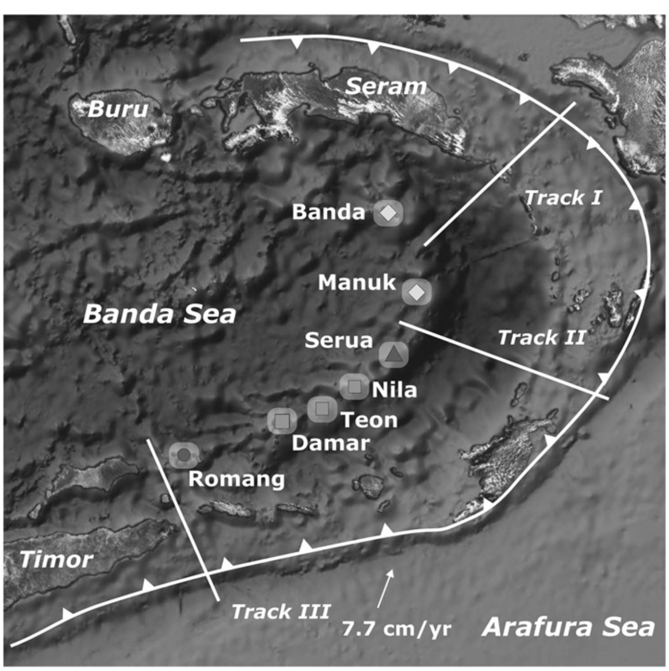

Fig. 1. Tectonic setting of the Banda Sea region. Exact sample localities are given in Vroon et al. (1993), and sediment track locations are taken from Vroon et al. (2001). Symbols for different islands are used throughout the manuscript. Subduction speed adopted from Fichtner et al., (2010).

also influenced by westward plate motions of the Pacific plate situated to the east (Bowin et al., 1980; Hall, 2002). The intra-oceanic arc encloses the Banda Sea and forms an almost 180° curve that is continued in the Sunda arc to the SW. Present-day tectonics around the Eastern end of the Sunda–Banda arc are characterised by the collision between leading portions of the passive Australian continental margin and the island arc that borders the Flores and Banda Seas (Fig. 1). The extent to which the continental margin has entered the subduction zone is unclear. McCaffrey (1989) estimated that the leading portion of the Australian continent was located at a depth of ~400 km in the Timor region, but more recent estimates suggest a complex decoupling and relocation of oceanic and crustal lithosphere with delamination of crustal units (Fichtner et al., 2010).

Volcanism in the Sunda–Banda arc ranges from an intra-oceanic arc environment (NE Banda) to arc volcanism dominated by a crustal input (Sunda) where a continental margin is being subducted (Elburg et al., 2004, 2005; Fichtner et al., 2010; Vroon et al., 1993, 1995, 2001). In the sampling area of the present study in the northeast of the Banda arc, the Banda Sea crust is essentially oceanic in nature (Hamilton, 1979) but different models have been proposed as to its age and origin. It has been regarded as a trapped Jurassic–Cretaceous piece of Indian Ocean crust (e.g., Bowin et al., 1980) or as a Cretaceous–Eocene marginal basin similar to the Sulawesi basin (Lee and McCabe, 1986). Geodynamic considerations (Hamilton, 1979) and dating of dredged samples (Hinschberger et al., 1999; Honthaas et al., 1998) support a Neogene back-arc origin.

Arc rocks from the Banda arc and the intersection with its western extension into the Sunda arc have long been known to be influenced by continental material (Bowin et al., 1980; Magaritz et al., 1978; Stolz et al., 1990; Vroon et al., 1993; Whitford and Jezek, 1979a). The subducting plate at the Banda arc is covered by variable amounts of continent-derived material, with predominantly Paleozoic–Precambrian sediments derived from New Guinea, Timor, and the Australian craton (Vroon et al., 1995). In contrast, the Banda arc itself is probably constructed on oceanic crust covered by 1–2 km of sediments (Hamilton, 1979), but distinction between subducted continental crust and subducted terrigenous sediments remains elusive. Hilton et al. (1992) argued for the involvement of continental crust to explain low $^{3}He/^{4}He$ of the Banda arc, and Elburg et al. (2004) proposed the involvement of lower continental crust in the inactive segment just west of the Banda arc towards the Sunda arc on the basis of Pb isotopes. Recent tomographic studies of the Banda Sea area also suggest subduction of continental material to depths exceeding 100 km (Fichtner et al., 2010).

Since it is difficult to geochemically distinguish between subducted continental crust and subducted terrigenous sediments, we use the term “subducted continental material” (SCM). Previous detailed Sr–Nd–Pb–O isotope investigations on Banda arc volcanic rocks and on sediments from the Australian–New Guinea shelf and accretionary wedge (Nebel et al., 2010b; Vroon et al., 1993, 1995, 2001) argued on the basis of bulk mixing between SCM and the mantle wedge that a contribution of up to 10 wt.% SCM is required to explain the observed isotopic variations.

Samples analysed for Zr–Hf–Lu concentrations and Hf isotopes (Table 1) were chosen from a suite with known major/trace-element abundances and Sr–Nd–Pb–O–He isotopes (Hilton et al., 1992; Hoogewerff et al., 1997; Vroon et al., 1993, 1995, 2001). The selection was based on location along the arc and minimal degrees of late-stage differentiation with samples ranging from basaltic andesites to dacites (Table 2, SiO_2 from ~50 to ~72 wt.%). The samples were collected from the Banda Archipelago (the active volcano Banda Api (BA) and the outboard island of Banda Neira, BN), Manuk (MA), Serua (SE), Nila (NI), Teon (TE), Damar (DA), and Romang (RO) (Fig. 1). Details of the locations of sampled islands and rock descriptions are given in Vroon et al. (1993).

Table 1
Concentrations of Lu, Hf, Zr and Hf isotope compositions of Banda arc volcanic rocks.

Sample	Group	Island	ppm Lu	ppm Hf	ppm Zr	Zr/Hf	$^{176}Lu/^{177}Hf$	$^{176}Hf/^{177}Hf \pm 2$.s.e.
BA11A2	Northern	Banda Api	0.6576	3.057	99.13	32.42	0.02950	0.283139 ± 14
BN3A2	Northern	Banda Neira	0.3959	1.659	52.96	31.91	0.03273	0.283101 ± 15
BN4A1	Northern	Banda Neira	0.5199	2.414	79.07	32.75	0.02954	0.283114 ± 13
MA2D	Northern	Manuk	0.4139	2.125	69.01	32.47	0.02672	0.283057 ± 04
MA5A	Northern	Manuk	0.4311	2.851	102.3	35.87	0.02074	0.283058 ± 17
MA6A1	Northern	Manuk	0.4326	2.915	105.1	36.06	0.02036	0.283050 ± 09
SE9A3	Central	Serua	0.3455	2.512	87.12	34.68	0.01887	0.282802 ± 15
SE21A	Central	Serua	0.3428	2.892	101.2	34.99	0.01626	0.282755 ± 03
SE25A	Central	Serua	0.3726	3.088	110.2	35.69	0.01655	0.282689 ± 15
NI1A1	Southern	Nila	0.4849	3.591	122.9	34.23	0.01852	0.282997 ± 11
NI9A	Southern	Nila	0.4001	3.363	115.3	34.30	0.01632	0.282996 ± 10
NI17A	Southern	Nila	0.5736	3.482	119.3	34.26	0.02260	0.282993 ± 10
NI18A1	Southern	Nila	0.2579	1.517	48.70	32.11	0.02332	0.283010 ± 12
TE1C	Southern	Teon	0.3195	3.440	123.8	35.98	0.01274	0.282812 ± 13
TE2B2	Southern	Teon	0.3235	2.805	94.82	33.80	0.01582	0.282899 ± 04
TE4B	Southern	Teon	0.3248	3.077	109.6	35.63	0.01448	0.282877 ± 12
TE15	Southern	Teon	0.3341	3.052	109.5	35.88	0.01501	0.282904 ± 16
DA1	Southern	Damar	0.3786	3.112	106.1	34.08	0.01668	0.282895 ± 16
DA9B	Southern	Damar	0.3491	3.138	108.7	34.65	0.01526	0.282908 ± 10
RO2	Extinct southern	Romang	0.3471	3.439	115.4	33.57	0.01385	0.282685 ± 04
RO8C6	Extinct southern	Romang	0.3844	3.983	114.0	28.62	0.01324	0.282676 ± 16
JB2-I	Standard	–	1.502	47.44	0.0340	31.58	0.03580	0.283221 ± 08
JB2-II	Standard	–	1.502	47.21	0.0350	31.43	0.03580	0.283197 ± 10
JB2-III	Standard	–	1.500	47.04	0.0364	31.35	0.03593	0.283198 ± 09
JB2-IV	Standard	–	1.501	49.16	0.0354	32.76	0.03583	0.283210 ± 08
JB2-V	Standard	–	1.505	47.51	0.0368	31.57	0.03588	0.283178 ± 10
JB2-VI	Standard	–	1.502	47.46	0.0341	31.61	0.03578	0.283179 ± 12

Errors on Hf isotope analyses are in-run precisions; external errors are ± 0.000014 based on repeated analyses of the JMC-475 standard solution (Nebel et al., 2009). Six splits of the standard reference material JB2 are taken from Nebel et al., 2010a.

The samples can be divided into four distinct groups (Fig. 1) based on their major element composition, Nd–Sr–O isotopes and location along the arc (Vroon et al., 1993, 2001). Group 1, the *northern arc*, comprises the islands of Banda Archipelago and Manuk. The second group is represented by the island of Serua and represents the *central arc* further to the south. The third group further south along-arc, here referred to as *southern arc*, consists of the islands of Nila, Teon and Damar. Group four, here labeled as *southern inactive arc*, includes the island of Romang, which is part of the inactive segment between the Banda arc and the East Sunda arc (Elburg et al., 2004, 2005; Van Bergen et al., 1993).

Table 2
Selected major element and isotopic data for samples used in this study, from Vroon et al. (1993, 2001).

Sample	wt.% SiO_2	wt.% MgO	$\delta^{18}O$ (melt)[a]	$^{143}Nd/^{144}Nd$
BA11A	59.14	3.52	5.78	0.51287
BN3A2	50.99	5.14	5.83	0.51284
BN4A1	53.70	3.27	n.d.	n.d.
MA2D	56.63	4.42	n.d.	n.d.
MA5A	55.29	4.78	5.97	0.51274
MA6A1	56.35	4.97	n.d.	n.d.
SE9A3	56.00	5.54	7.19	0.51249
SE21A	59.81	4.02	7.12	0.51244
SE25A	59.26	4.24	7.48	0.51240
NI1A1	57.92	3.08	5.92	0.51263
NI9A	57.68	3.45	n.d.	n.d.
NI17A	57.80	3.01	n.d.	n.d.
NI18A1	51.93	5.39	5.84	0.51267
TE1C	59.94	2.63	6.48	0.51252
TE2B2	54.79	5.14	n.d.	n.d.
TE4B	57.86	3.23	n.d.	n.d.
TE15	58.43	2.85	6.18	0.51258
DA1	56.67	3.50	6.03	0.51257
DA9B	56.63	3.75	n.d.	n.d.
RO2	58.93	4.63	8.82	0.51248
RO8C6	71.61	0.31	6.13	0.51243

[a] $\delta^{18}O$ is the deviation of the calculated isotope composition of the melt (see Vroon et al., 2001 for details) expressed in the deviation per 1000 from SMOW.

3. Analytical protocol

Approximately 100 mg of sample material were weighed and doped with a mixed ^{94}Zr–^{176}Lu–^{178}Hf–^{180}Ta isotope tracer, and dissolved in a HF-HNO_3 (5:1) acid mixture. All powders were dissolved on a hot plate at 130 °C for 24 hours and evaporated to dryness. The samples were treated with concentrated HNO_3 and traces of HF to break down fluorides until a clear solution was achieved. Subsequently, after samples were converted into a chloride form with 6 M HCl, a 5% aliquot was saved for future trace element analyses in conjunction with Ta isotope dilution analyses. Acids used in the present study were double Teflon distilled except for HF, which was distilled once to avoid the accumulation of volatile TaF_5. Details of the spiking, and Lu, Hf, and Zr purification procedures are given elsewhere (Münker et al., 2001; Nebel et al., 2009).

Isotope analyses of Lu, Hf, and Zr, and Hf isotope measurements were carried out on a ThermoFinnigan Neptune multi-collector-ICP-MS at VU University Amsterdam. Details of the instrumental configuration and analytical procedures are given in Morel et al. (2008) and Nebel et al. (2009). To cross-check the precision and accuracy of our methods rock reference materials JB-1, JG-1, BHVO-2, and BCR-2 were also analysed for HFSE abundances and Hf isotope compositions (see Nebel et al., 2009, 2010a, 2010b). The JMC-475 standard solution yielded a mean value of $^{176}Hf/^{177}Hf = 0.282168 \pm 6$ ($n = 9$), and all Hf isotope values were reported relative to $^{176}Hf/^{177}Hf = 0.282160$ (Blichert-Toft et al., 1997). Procedural blanks during the course of this study were 10 pg, 15 pg, and 45 pg for Lu, Hf and Zr, respectively.

4. Results

4.1. Zr–Hf–Lu abundances

Zirconium, Hf, and Lu contents of Banda arc samples are given in Table 1. Concentrations are within the published range of island arc rocks (Kelemen and Hanghoy, 2003) with 49–124 ppm Zr, 1.5–4.0 ppm Hf, 0.26–0.66 ppm Lu, and an average Zr/Hf of 34 ± 4 (2 s.d.).

Lutetium–hafnium ratios of the rocks vary from $^{176}Lu/^{177}Hf = 0.033$–0.013, spanning a range from close to depleted mantle values (0.038; Chauvel and Blichert-Toft, 2001) to crustal values (0.0093; Vervoort and Patchett, 1996).

There is no systematic variation in Zr/Hf or Lu/Hf with the degree of differentiation as monitored by wt.% MgO (Fig. 2). The increasing involvement of crustal components along the arc, as previously inferred from O–Sr–Pb isotopes (Vroon et al., 1993, 2001), appears to be reflected in the change in Zr/Hf (Fig. 2) and the decrease in HREE/HFSE (expressed here as $^{176}Lu/^{177}Hf$), which also correlate with the position of the samples along the arc from NE to SW (Table 1).

4.2. Hafnium isotopes

The Hf isotope results for 21 whole-rock samples are presented in Table 1, together with previously published O and Nd isotope data (Table 2). The northern Banda arc volcanoes (Banda Archipelago and Manuk) have high $^{176}Hf/^{177}Hf$ ratios with limited variation (0.28314–0.28305), whereas Serua in the central part displays a large range in Hf isotopes (0.28280–0.28269). This range overlaps with results for two Serua samples previously analysed by (White and Patchett, 1984). The southern arc samples (Nila, Teon, Damar) have low and variable Hf isotope ratios (0.28301–0.28268). The southern inactive arc (Romang) has the lowest $^{176}Hf/^{177}Hf$ values of 0.28268 and 0.28269.

The Hf isotope data of volcanic rocks from the Banda arc show a correlation with Nd isotopes typical for island arc related igneous rocks, and broadly overlap with the mantle array (Fig. 3A). In detail, the Banda samples are offset towards higher $^{176}Hf/^{177}Hf$ at a given $^{143}Nd/^{144}Nd$ compared to the global crust–mantle array, and in Hf–Nd isotope space the samples plot on a trend towards the Indian-type MORB field (ITM, Fig. 3B). Excluding Serua, the Hf isotope ratios decrease from NE to SW along the Banda arc. This trend is similar to that displayed by Nd isotopes (Vroon et al., 1993). The northern arc exhibits $^{176}Hf/^{177}Hf$ overlapping with other intra-oceanic arcs such as the Honshu arc. In contrast, the rock series further south has less radiogenic Nd–Hf isotope ratios that define trends that overlap with other oceanic island arcs such as the Lesser Antilles (Fig. 3A). In summary, the Hf isotope data record a clear spatial variation along the arc decreasing from NE to SW.

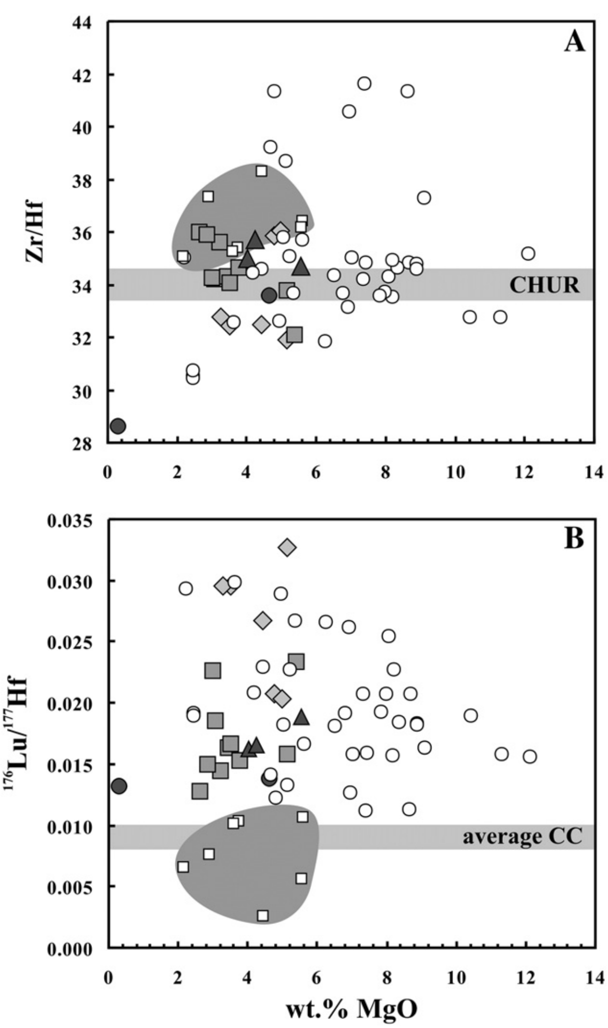

Fig. 2. Zr/Hf (A) and Lu/Hf (B) of the Banda arc volcanic rocks versus wt.% MgO. Kamtchatka arc volcanics (open circles), which span a larger range in MgO than the Banda arc, are plotted for comparison. The former are influenced by no or only little sediment contribution to the source of the arc rocks (Münker et al., 2004). There is no systematic variation of the Banda rocks with MgO pointing to no effects of fractional crystallisation on the Zr/Hf and Lu/Hf. The grey field highlights adakites (open quadrates, Münker et al. 2004). Average continental crust (CC) after Vervoort and Patchett (1996). CHUR value taken from Münker et al. (2003).

5. Discussion

5.1. The role of assimilation and fractional crystallisation (AFC)

Assimilation of existing arc crust during magma ascent can have large effects on isotope and elemental abundances of newly formed arc rocks, and such effects can be similar to those caused by SCM contribution to the magma source (e.a., Arculus and Powell, 1986; Hawkesworth et al., 1993; McCulloch and Gamble, 1991; Thirlwall et al., 1996; Woodhead et al., 1998). Previous studies based on

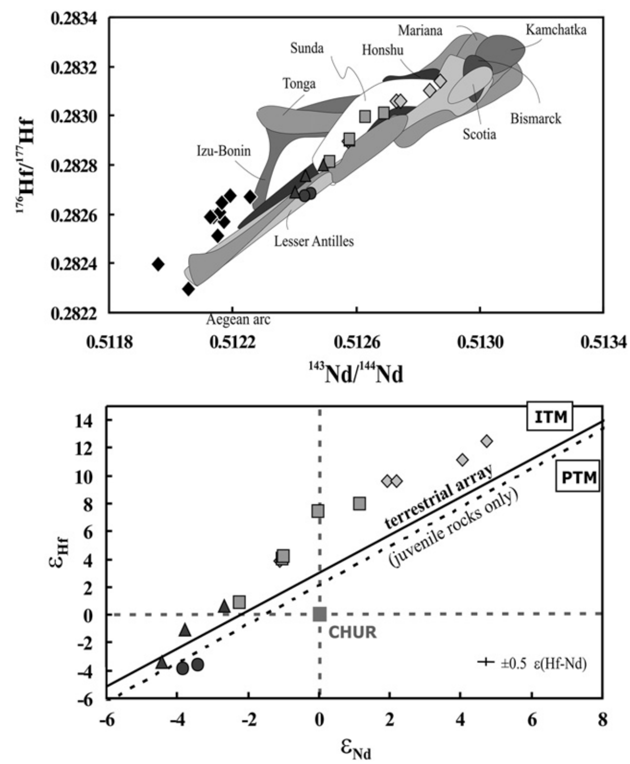

Fig. 3. Hf–Nd isotope diagram of Banda arc rocks in comparison with other island arcs (georoc database: http://georoc.mpch-mainz.gwdg.de/georoc/). A) The Banda arc displays decreasing $^{176}Hf/^{177}Hf$ and $^{143}Nd/^{144}Nd$ from NE to SW along arc. Sediments from the accretionary wedge and the Australian–New Guinea shelf (average East Indonesian Sediments = E.I.S.) are shown for comparison as black diamonds (Nebel et al., 2010b). Data from Tables 1 and 2. Symbols for arc rocks are as in Fig. 1. B) The epsilon notation represents the deviation of a sample from the chondritic uniform reservoir times 10,000 (Bouvier et al., 2008). Terrestrial array after Vervoort and Blichert-Toft (1999); juvenile array shows data for ITM/PTM = Indian/Pacific type mantle, after Pearce et al. (2007).

petrography and Sr–Nd–Pb–O isotopes of Banda arc volcanic rocks reported that assimilation of arc crust is an important process in the central arc segment at Serua (Jezek and Hutchinson, 1978; Magaritz et al., 1978; Morris et al., 1984; Vroon et al., 2001). Vroon et al. (2001) argued on the basis of O and Sr isotopes that Serua can be divided into three groups. One group is not influenced by AFC processes with $\delta^{18}O$ <7, whereas another group with $\delta^{18}O$ >7 experienced substantial arc crust assimilation. An intermediate group probably reflects a mixing of the two former groups (Vroon et al., 2001). Our Serua samples exhibit high $\delta^{18}O$ (7.1–7.5‰) and are thus affected by AFC, which is in agreement with low $^{176}Hf/^{177}Hf$ (0.282689–0.282802). We therefore excluded the central arc segment from the discussion below on source mineralogy and mixing processes between mantle and SCM.

Volcanic rocks of the southern inactive arc at Romang are characterised by variable $\delta^{18}O$ and non-radiogenic Hf–Nd and radiogenic Sr isotope signatures. Elburg et al. (2005) and Vroon et al. (2001) interpreted these rocks as not being influenced by AFC processes based on thin sediment layer (~1 km) in that area (Hamilton, 1979). Instead, the geochemical signatures of Romang lavas are interpreted as being caused by mixing of melts derived from subducted continental crust with the mantle wedge at depth (Vroon et al., 1995, 2001). Hence, further investigation on the influence of SCM will focus on the northern and southern arc segments, with the central and southern inactive arc as monitors for either assimilation from arc crust or melt contribution from continental crust.

Magmatic fractionation cannot affect Hf isotope compositions but can influence elemental abundances and ratios. In the present study, Zr/Hf and Lu/Hf are used to constrain the source of Hf isotope signals. As such, any interpretation regarding SCM parameters on the basis of these elements can be flawed by arc-related fractionation processes. In the case of the Banda arc samples, we selected rocks that have a narrow range of fractionation as indicated by a narrow range in wt.% MgO (Table 2, ranging from 2.6 to 5.5, excluding the highly differentiated sample RO8C6). Within these limits, no systematic variations of Lu/Hf or Zr/Hf with MgO are observed (Fig. 2), such that Lu/Hf and Zr/Hf are evidently not influenced by differentiation.

5.2. Hf–Nd interactions between mantle wedge and SCM component

The mantle wedge beneath the Banda arc is composed of a depleted ITM, as inferred from the Hf–Nd isotope trend in Fig. 3 and based on the tectonic configuration of the Banda Sea that implies an entrapped piece of oceanic Indian oceanic crust (e.g. Bowin et al., 1980) or back arc basin (e.g. Honthaas et al., 1998). We assume this ITM source to be depleted in trace elements based on sub-chondritic Zr/Hf (32–33) in the isotopically most radiogenic samples of the northern Banda arc (Table 1, Fig. 2), which requires a depleted mantle source (e.g., Weyer et al., 2003).

Sediment samples from three tracks from the Australian–New Guinea shelf and the accretionary wedge that are representative for SCM subducting underneath the Banda arc (track locations indicated in Fig. 1) have previously been studied in detail for their Hf–Sr–Nd–Pb–O isotopes and trace elements (Nebel et al., 2010b; Vroon et al., 1995, 2001). These sediments show a good correlation between $^{143}Nd/^{144}Nd$ and $^{176}Hf/^{177}Hf$ (Nebel et al., 2010b), and broadly follow the terrestrial array (Vervoort and Blichert-Toft, 1999). The $^{176}Hf/^{177}Hf$ in the track I and II samples are more radiogenic than samples from track III. These Hf isotope values fit with the observation that sediments from track III are derived from the old Archaean and Proterozoic terranes of the Australian continent, in line with previous Pb isotope investigations (Elburg et al., 2004; Vroon et al., 1995). In contrast, the northern part of the Australian shelf receives sediments from the Paleozoic terrains of New Guinea with more radiogenic Hf and Nd and lower Pb isotope ratios (Nebel et al., 2010b; Vroon et al., 1995).

The Hf and Nd isotope data display a general trend from an ITM source in the northern Banda arc towards non-radiogenic values in the southern part. As previously suggested by other authors (Vroon et al., 1993, 2001; Whitford and Jezek, 1979b) and by using the constraints on mantle wedge and SCM endmembers outlined above, this trend is broadly explained by bulk mixing of average subducting SCM material of <2 wt.% in the NE towards >2 wt.% in the SW and a depleted mantle wedge (Fig. 4A). However, in more detail, Banda rocks deviate slightly from a bulk mixing curve in Hf–Nd isotope space that is based on average Hf–Nd endmember concentrations with a Nd/Hf = 6.8. A mixing line forced through the arc rocks requires a Nd/Hf = 5, for which excess Hf relative to Nd is needed, or the retention of Nd relative to Hf. Experiments have shown that at pressures and temperatures relevant for subduction zone settings (i.e., ≥700 °C, 4 GPa) the mobility of Hf in fluids in equilibrium with eclogitic metasediment is three times less than that of Nd (Kessel et al., 2005), which excludes selective fluid mobility as the cause of the low Nd/Hf.

The relative mobility of Hf and Nd in melts is a function of source mineralogy (e.g., Yogodzinski et al., 2010). Garnet is likely to be a

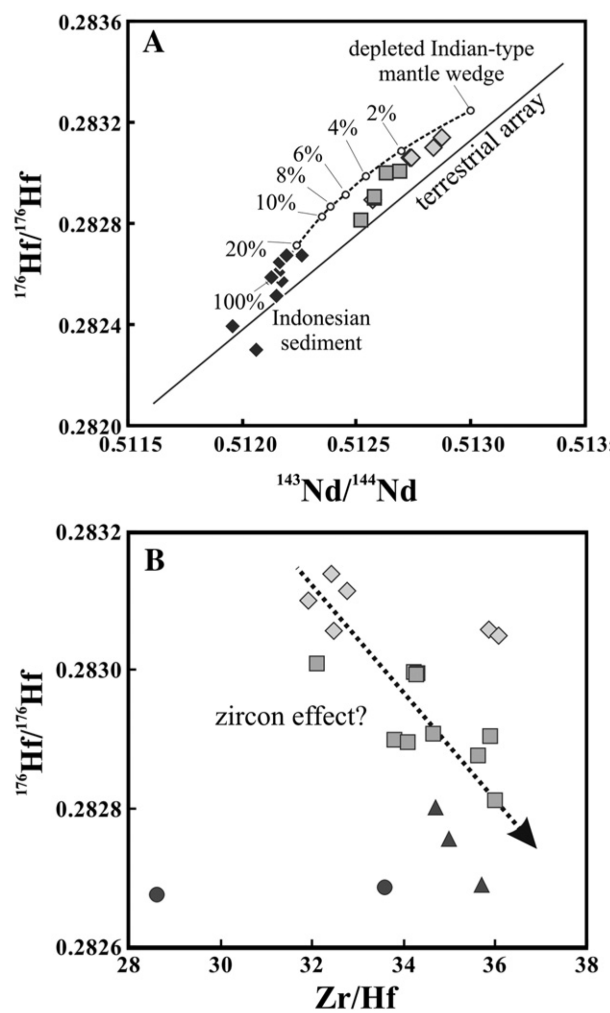

Fig. 4. A: Nd–Hf isotope mixing line between a depleted Indian-type mantle wedge (assumed to be Nd/Hf = 4, 0.25 ppm Hf and 1.0 ppm Nd; $^{176}Hf/^{177}Hf$ = 0.28325, $^{143}Nd/^{144}Nd$ = 0.51300) and average East Indonesian sediment (Nd/Hf = 6.8, 6.8 ppm Hf and 26 ppm Nd; $^{176}Hf/^{177}Hf$ = 0.28256, $^{143}Nd/^{144}Nd$ = 0.51212; after Vroon et al., 1995, Nebel et al., 2010b). A forced mixing trend to fit the Banda arc data requires Nd/Hf ~ 5. B: The systematic decrease of Hf isotope compositions of the arc rocks with increasing Zr/Hf indicates the contribution of a zircon-like component to the source region of the rocks.

residual phase after partial melting of an eclogitic assemblage that results from metamorphic processes acting on subducted sediment in subduction zones. Garnet-melt partition coefficients for Hf and Nd are subequal, and as such garnet does not qualify as a residual phase to significantly lower Nd/Hf (van Westrenen et al., 2001). In contrast, lower Nd/Hf can be achieved by partial melting accompanied by the breakdown of zircon, which elevates Hf concentrations relative to Nd. Likewise, the dominance of non-radiogenic Hf from zircon can be expected to shift Hf isotopes towards lower values for a given Nd isotope signal, which is a feature observed for the Banda arc. Hence, the Hf–Nd isotope co-variations raise the question whether zircon is contributing to the melts in the Banda arc.

5.3. The role of residual zircon during SCM melting

Hafnium isotope systematics indicate that addition of SCM to the southern segment of the Banda arc is different to the northern segment. The same systematics can be observed for Lu/Hf and Zr/Hf, which are both elemental ratios that are sensitive to a source mineralogy dominated by garnet and/or zircon. The $^{176}Lu/^{177}Hf$ vs. $^{176}Hf/^{177}Hf$ trend shown in Fig. 5 requires fractionation of Lu/Hf, which can be best explained by hydrous partial melting of SCM. Recent experimental studies of partial melting of sediments under P–T conditions relevant for magma generation beneath arcs show that residual garnet is present up to 20% melting (Hermann and Rubatto, 2009). The stability of zircon at high P–T conditions is less clear. Garnet retains HREE and controls the Lu budget of partial melts such that partial melts of sediment with residual garnet exhibit low Lu/Hf. There is growing evidence from arcs, which are traditionally considered to be fluid dominated as e.g., the Aleutians, that in these settings sediments are also melting (Yogodzinski et al., 2010). In these settings (see Fig. 5), the Lu/Hf is considerably lowered as a function of residual garnet, but the Hf isotope composition is barely affected (fluid-dominated arc rocks in Fig. 5A).

In contrast, zircon is the controlling mineral for Hf and its dissolution can supply large amounts of Hf from the sediment to a partial sediment melt, resulting in even lower Lu/Hf accompanied by a decrease in Hf isotope composition. Both of these features are observed at the Banda arc. This suggests that the dominant carrier of non-radiogenic Hf in the Banda arc might have been zircon, such that the coupled decrease in Lu/Hf and Hf isotope composition is at least partially caused by zircon dissolution. In the same way, decreasing $^{176}Hf/^{177}Hf$ along the arc coarsely define an anti-correlation with elevated Zr/Hf (Fig. 4B); both features that are attributed to zircon (e.g., Claiborne et al., 2006). Combined with high concentrations in zircon that will dominate the Zr and Hf budget in a sediment melt being added to a depleted, sub-chondritic mantle wedge (Weyer et al., 2003), this suggests a zircon signature in arc melts. This coupled along-arc trend is interpreted here as an additional indicator for progressive increase in zircon signals in the Banda arc rocks from NE to SW.

The combined effects of residual garnet and dissolution of zircon on $^{176}Lu/^{177}Hf$ are modeled in Fig. 5. Models using an eclogitic composition (assumed modal proportions: grt:0.39; cpx:0.3, mica:0.3, rutile:0.01, zrc:0.001; see Table 3 for partition coefficients, D) for subducted sediment (e.g., Rubatto and Hermann, 2007) indicate that the trend in Lu/Hf vs. Hf isotope composition in the Banda sample suite can be generated by a partial sedimentary melt accompanied by full dissolution of zircon (D = 0) and residual garnet (mixing line ‘a’ in Fig. 5). In a scenario with residual zircon ($D^{Hf} = 3476$, taken from Rubatto and Hermann, 2007), the Lu–Hf systematics of the Banda suite cannot be reproduced (mixing line ‘b’ in Fig. 5). The trend towards lower $^{176}Hf/^{177}Hf$ from NE to SW along the Banda arc can be explained by i) subducting zircons in the SW having less radiogenic $^{176}Hf/^{177}Hf$, since they are derived from Archaean and Proterozoic northern Australia and ii) more zircon has been added to the sediment melts in the SW part of the Banda arc because of either higher slab surface temperatures or more mature subducting sediments.

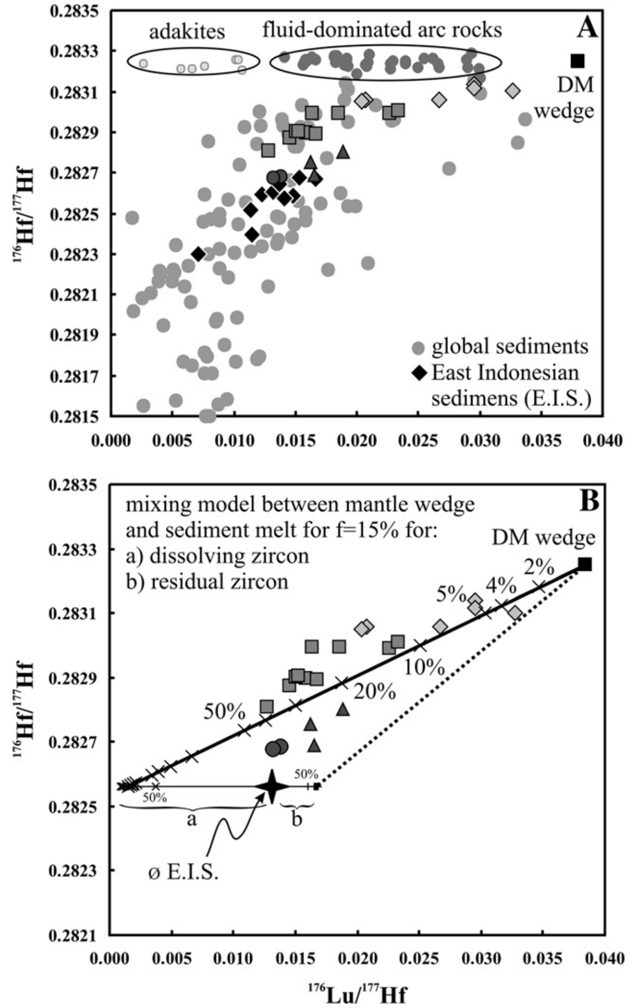

Fig. 5. A: Lu–Hf isotope evolution diagram of the Banda rocks. The NE–SW along-arc transect records a positive correlation (Serua and Romang excluded). This suggests a two component mixing of a component with $^{176}Lu/^{177}Hf < 0.01$ and $^{176}Hf/^{177}Hf < 0.2827$ and a depleted mantle source component in the mantle wedge. Adakites and arc rocks from the Kamchatka arc (Münker et al., 2004), and the Troodos Ophiolite Boninitic rocks (König et al., 2008) representing rocks with presumably no sediment in their source display a similar decrease in Lu/Hf with uniform, mantle-like Hf isotope compositions. Grey dots are global sediments (Vervoort et al., 1999), Black diamonds are East Indonesian sediments (Nebel et al., 2010b). B shows a mixing model of partial sedimentary melts (with f = 15%, batch melting) with a mantle wedge (Table 3). Crosses on mixing lines indicate percentages of mixing. Sediment melt a represents average East Indonesian Sediment (E.I.S. with $^{176}Lu/^{177}Hf = 0.013$ and $^{176}Hf/^{177}Hf = 0.28256$; Nebel et al., 2010b) with zircon entering the melt (assuming $D[Hf]^{zircon/melt} = 0$ and bulk D[Lu] = 3.29, bulk D[Hf] = 0.227); Melt b represents a sediment melt derived from EIS with residual zircon (bulk D[Lu] = 3.91, bulk D[Hf] = 5.08); see Table 3 for modelling parameters. The dashed lines indicate mixing between a depleted mantle source and the melt with residual zircon, which cannot account for the observed arc rock signatures.

5.4. Geodynamic and geochemical constraints on zircon dissolution

The dissolution of zircon in a sediment melt is governed by zircon saturation, i.e., Zr solubility in the melt, which increases with temperature (Watson and Harrison, 1983) and possibly decreases with pressure (Rubatto and Hermann, 2007). Zirconium solubility in melts further changes with melt composition, which will vary with degree of melting. Tollstrup and Gill (2005) calculated Zr solubility in a granitic melt using parameters given in Watson and Harrison (1983), and suggest that for a subducted sediment containing 65–165 ppm Zr, temperatures need to be lower than 780 °C for zircon to

Table 3
Parameters used in mixing models of Figs. 3 and 5.

Figure 3			
	DMM	Sediment	Arc crust
ε_{Hf}	16	−7	−5
$\delta^{18}O$	5.7	18.7	9.8
ppm Hf	0.2	3.8	4
ppm O	438000	502000	502000
Figure 5			
Mineral	wt.%	D (Lu)	D (Hf)
Zircon	0.001	445	3467
Garnet	0.39	7.1	0.24
Cpx	0.3	0.449	0.2
Phlog	0.3	0.0016	0.016
Rutile	0.01	0.016	4.61

Note: $^{176}Lu/^{177}Hf$ of the sediment end member is 0.013 (3.8 ppm Hf; 0.35 ppm Lu) and $^{176}Hf/^{177}Hf$ is 0.28256 based on average East Indonesian sediment (Nebel et al., 2010b). References for D values follow the suggestion of Todd et al., 2010 and are: zircon: Rubatto and Hermann (2007), rutile: Foley et al., 2000; cpx/grt: Johnson, 1998, phlogopite: Adam and Green, 2006.

survive. This conclusion is in agreement with experiments by Johnson and Plank (1999), who report sediment melting at 780–825 °C for per- to meta-aluminous melts at 3–4 GPa. Recent slab surface temperature estimates from the Izu arc in regions where melt is generated vary between 830 and 890 °C (Tollstrup et al., 2010), exceeding the temperatures anticipated for zircon dissolution. Sediments that are representative for SCM have Zr concentrations within the range considered by Tollstrup and Gill (2005) (~150 ppm on average, carbon-free, Nebel et al., 2010b). These parameters generally favor zircon dissolution in the source of Banda arc magmas.

In contrast, Johnson and Plank (1999) report secondary evidence for the possible survival of zircon in their experimental per-aluminous melts at high temperatures, in agreement with Klimm et al. (2008), who identified stable zircon at ~850–900 °C in experimental hydrous basaltic melts. Most recently, Hermann and Rubatto (2009) performed experiments with material of variable silica contents and show that temperatures need to exceed 925 °C for felsic melt to fully dissolve zircon. For the Banda arc, it is unclear if this temperature is achieved. The required temperature appears high compared to many estimates of the thermal structure of the subduction zone, although there is growing evidence for slab surface temperatures exceeding 925 °C (e.g. Plank et al., 2009).

Models for the East Banda Sea (Syracuse et al., 2010) show a wide range of predicted slab surface temperatures compared to other arcs, although the absolute value is strongly model dependant (~710–910 °C). This temperature range is on average ~50 °C below that required according to Hermann and Rubatto (2009) to fully dissolve zircon in the southern part of the Banda arc. A possible source for the extra heat required could be slab detachment, whereby hot asthenospheric mantle heats up the edges of the continental plate in the gap between the detached sinking oceanic plate and the edge of the subducted Australian continental plate. However, evidence for slab detachment has not been found in a recent tomographic study by Fichtner et al. (2010), and adakitic melts, which can occur at the edge of slabs, have not yet been reported for the Banda region. Following the geochemical constraints outlined above, and if our interpretation of total zircon dissolution based on Hf isotopes and Lu–Zr–Hf systematics is correct, the slab surface temperature should exceed 925 °C.

5.5. The effect of sediment recycling on Hf–O isotope co-variations

Mixing of isotope domains is long known to be a problem in Nd model age calculations (Arndt and Goldstein, 1987), and has been discussed in some detail for Hf in conjunction with zircon model ages (e.g., Hawkesworth and Kemp, 2006; Kemp et al., 2006). Hafnium model ages of crustal rocks and their constitute minerals, most notably zircons, have been widely used to estimate the timing of juvenile crust formation and crustal growth (e.g., Hawkesworth et al., 2010 and references therein). However, similar to Nd model ages, these Hf model ages are geologically meaningful only if the host magma lacked a mixed or sedimentary source component (Arndt and Goldstein, 1987); if not, then they provide a hybrid age of multiple components. This hybrid age problem can be potentially circumvented by combining Hf–O isotope systematics of zircon, given that zircon O isotopes are considered sensitive to sediment contribution (e.g., Hawkesworth and Kemp, 2006; Kemp et al., 2006, 2007; Pietranik et al., 2008). For instance, Kemp et al. (2006) distinguished a series of crust formation episodes for Eastern Gondwana on the basis of Hf model ages deduced from zircons with $\delta^{18}O<6.5$, assuming that their host melts contained minor or negligible amounts of sediments. Our comprehensive geochemical and isotopic data sets from the Banda arc allow us to evaluate the validity of this assumption for Hf model age calculations.

Oxygen isotopes have previously been used to trace and quantify crustal components in island arc environments (e.g., Eiler et al., 2000; Turner et al., 2009; Vroon et al., 2001). For the Banda arc, Hf–O isotope systematics (Fig. 6A) display a progressive increase in crustal involvement from the northern to the southern arc, and sediment addition in the northern and southern arc segment varies from ~1% to ~10%, respectively. These percentages broadly overlap with the suggested ranges of sediment inputs for the Lesser Antilles islands of Grenada and Martinique (1–8%) based on Hf–Nd isotopes (Carpentier et al., 2009), and earlier mixing models with Nd–O isotopes for the Banda arc (Vroon et al., 2001).

These mixing relationships have consequences for zircons forming out of these melts, which are considered to be in O *and* Hf isotope equilibrium with their host melt, noting that $\delta^{18}O$ of a zircon is even ~0.5–2‰ lower than that of its host whole-rock (Valley et al., 2005). For the Banda rocks, there is only little variation in $\delta^{18}O$ of 5.8–7.5‰, which contrasts with the substantial changes in Hf isotopes ($\varepsilon_{Hf}=-3.8$ to 12.5) (Fig. 6B). These observations demonstrate that ~10% sediment addition can generate a magma having highly non-radiogenic Hf isotopic signatures with restricted elevation of $\delta^{18}O$. Hence, the oxygen isotope composition of the Banda samples (and by extension of zircons forming in them and other convergent plate margins) suggests an origin in a mildly evolved, juvenile crust. In contrast, the Hf isotope compositions clearly reveal the involvement of a mature crustal component.

These results clearly indicate that zircons and other phases that formed in convergent margin settings with $\delta^{18}O<6.5$ can exhibit mixed, and by this significantly older Hf model ages. Hence, such crust formation model ages should be applied to sedimentary provenance studies or models of crustal growth with great caution.

5.6. Implications for Hf isotopes in the Hadaean detrital zircon record

The earliest terrestrial zircon record is dominated by non-radiogenic $^{176}Hf/^{177}Hf_{(t)}$ (negative ε_{Hf}) (Blichert-Toft and Albarede, 2008; Harrison et al., 2005, 2008; Kemp et al., 2010; Nebel-Jacobsen et al., 2010). This points to crustal reservoirs that existed for hundreds of millions of years with a low Lu/Hf with respect to Bulk Silicate Earth (BSE) consequent to internal crustal reworking (Kemp et al., 2010). An alternative explanation for these non-radiogenic Hf isotope compositions, borne out by our Banda arc results, invokes the onset of plate tectonic activity ~4.4 Ga ago and the associated formation of new crust at convergent plate boundaries (Harrison et al., 2008; Hopkins et al., 2008; Menneken et al., 2007). Although the nature of Archaean and possibly even Hadaean subduction zone activity remains elusive, associated crustal recycling potentially shares two fundamental similarities to present-day subduction systems: (1) A

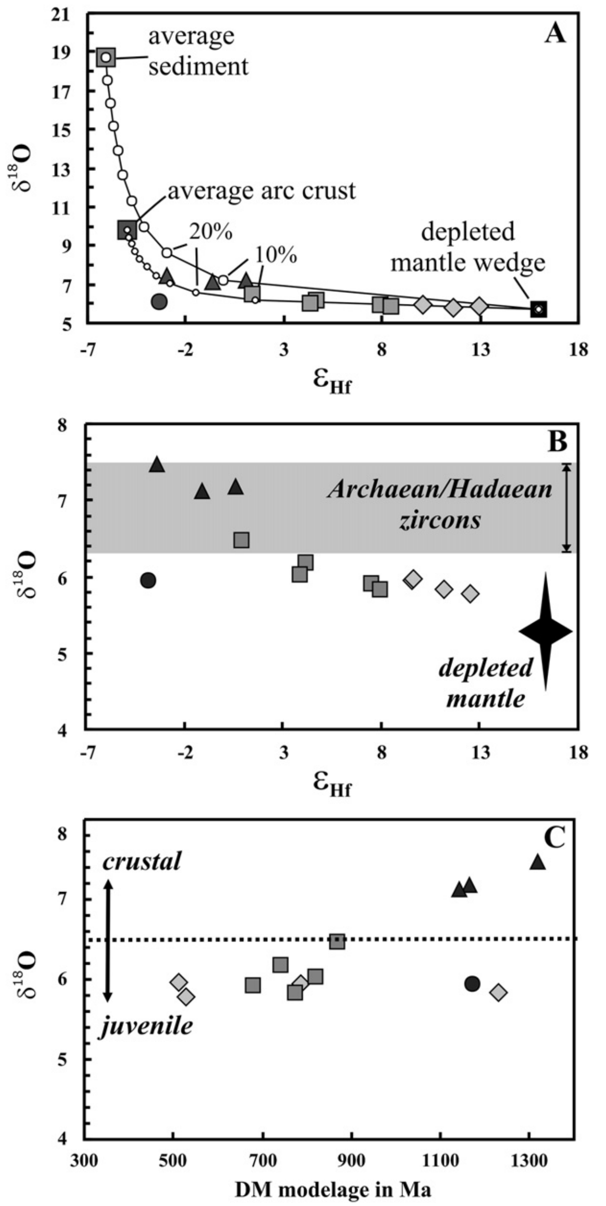

Fig. 6. A: Oxygen isotope compositions of Banda arc samples as reported in (Vroon et al., 2001) vs. Hf isotope compositions (this study), indicating a mix between a depleted mantle wedge source and SCM/arc crust. B: Detail of the Banda samples in comparison with the range observed for Archaean/Hadaean zircons (Valley et al., 2005) and depleted mantle values (after Chauvel and Blichert-Toft (2001) and Cavosie et al. (2009), indicating that Hadaean zircons could have formed in an subduction-related environment. C:Oxygen isotope data for the Banda arc vs. Hf model age (in Ma) showing the large range in model ages for a relatively narrow range in δ^{18}O.

subducted mineral assemblage typical for convergent plate boundaries (Hopkins et al., 2008, 2010; Menneken et al., 2007), and (2) surface weathering in the presence of liquid water that allowed sediment transport to subduction zones (Harrison, 2009; Mojzsis et al., 2001; Trail et al., 2007; Ushikubo et al., 2008; Valley et al., 2002). A considerable difference between Archaean/Hadaean and present-day subduction zones is the predominant subduction of buoyant, hot plates with higher temperature ranges (Foley, 2008) with subduction velocities probably similar to present-day values (Hopkins et al., 2010). These conditions would enhance the preferential melting of subducted sediments.

Our data show that subduction of sediments can result in the recycling of their non-radiogenic Hf isotope character. By implication, the mixed Hf isotope signal of crustal and juvenile material can be preserved in newly formed zircons in new, most probably felsic arc crust (Fig. 7). Such 'second-generation-Hf' zircons will not fall on the expected Hf isotope vs. time line trend that is generally believed to record repeated intracrustal reworking of a primary crust (Kemp et al., 2010). Hence, deviations from a straight array that is expected for re-melting of crust in Fig. 7 may thus indicate the involvement of sediment during subduction activity.

Hence, we propose that the combination of (1) early formation of a low Lu/Hf proto-crust, (2) initiation of subduction shortly thereafter and (3) subsequent crustal reworking coupled with the recycling advocated here, is a feasible mechanism to explain the Hadaean Hf isotope record. Such a scenario is also in agreement with Li isotope compositions in Hadaean zircons that require surface-exposed crustal components in the source of these zircons (Ushikubo et al., 2008). Both Li and Hf could have been derived from a sedimentary partial melt, with its isotopic signature preserved in the zircons. This model requires the onset of subduction activity as early as ~4.4 Ga, and implies that sediment melting by steeper geotherms was a common process in the Hadaean.

Sediment recycling in a subduction setting can further account for Hf–O isotope co-variations in the Hadaean zircon record. The narrow range in O isotopes reported for Hadaean zircons is believed to reflect infant stages of continental crust (Cavosie et al., 2005; Mojzsis et al., 2001; Peck et al., 2001; Valley et al., 2005; Wilde et al., 2001). However, this model is at odds with the large range in non-radiogenic Hf isotope ratios reported in the Jack Hills zircon record (Blichert-Toft and Albarede, 2008; Harrison et al., 2005, 2008; Kemp et al., 2010; Nebel-Jacobsen et al., 2010), for which a mature crust is required. An initially mafic crust derived from a mantle source that is only slowly evolving towards continental crust signatures with low δ^{18}O values is expected to have moderate Lu/Hf and as such more radiogenic, i.e., mantle-like Hf isotope compositions.

Primary magmatic Hadaean zircons exhibit a narrow range in δ^{18}O (6.3–7.5 ‰) (Cavosie et al., 2005; Harrison et al., 2008; Mojzsis et al., 2001; Peck et al., 2001; Trail et al., 2007; Valley et al., 2005) that exceeds upper mantle values of 4.5–6.1‰ (Cavosie et al., 2009). These data overlap with the range of δ^{18}O of the Banda arc samples demonstrating that O isotope signals as recorded in the Hadaean zircons are consistent with formation in a convergent margin setting with reworking of older crust by SCM recycling (Fig. 6B).

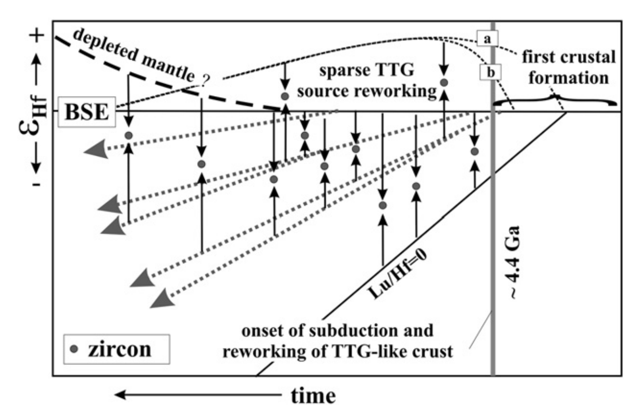

Fig. 7. Schematic sketch of Hf isotopes vs. time illustrating the effect of crustal reworking on Hadean Hf isotopes-in-zircon during zircon crystal growth in a subduction-related tectonic setting: Hf isotopes (expressed in ε_{Hf} notation) in zircons (dots) constitute a mixture of a reworked component and a mantle source. The mantle source either represents the bulk silicate Earth (BSE) before ~4.0 Ga, or the depleted mantle (after ~4 Ga). Dashed curved lines a) and b) denote different times for the onset of subduction zone activity associated with crustal reworking of mafic, garnet-bearing successions. BSE = bulk silicate Earth.

Reworking of proto-crust in hot subduction zones with geothermal gradients similar to those observed at the Banda arc can readily account for the observed Hf–O isotope patterns in the Hadaean zircon record. We note that sediments derived from evolved crust are required in such a scenario, which might be a delimiting factor and in favor for a scenario without subduction activity. Such a static tectonic setting that is also capable of creating the observed Hf isotope patterns is observed on the Moon (Taylor et al., 2009), where subduction and evolved continental crust are evidently absent. However, although Hadaean lunar zircons show Hf isotope patterns similar to those of their terrestrial counterparts (Kemp et al., 2010), their $\delta^{18}O$ overlap with mantle values (Nemchin et al., 2006), unlike the terrestrial zircons. This strongly suggests that an early subduction scenario is more likely for the Hadaean Earth than a static lunar model without subduction.

6. Conclusions

The Lu/Hf, Zr/Hf and Hf–Nd isotope systematics of the Banda arc demonstrate that the amount of subducted continental material increases along the arc from <2% in the NE to >2% in the SW. The systematic change in Hf isotope compositions confirms that HFSE (Hf) can be mobile in a subduction setting, as previously reported for other arcs (Barry et al., 2006; Marini et al., 2005; Todd et al., 2010; Tollstrup and Gill, 2005; Tollstrup et al., 2010; Yogodzinski et al., 2010). Hydrous fluids do not qualify as an agent to affect Nd/Hf to reproduce the Hf–Nd isotope signatures of the arc rocks. In contrast, hydrous partial sediment melts with Nd/Hf of ~5 are inferred as the transport medium in the southern part of the arc.

The Lu/Hf and Zr/Hf systematics require garnet as a residual mineral and at least a partial contribution from subducting zircon during sediment melting. Following experimental constraints, this requires <20% degree of melting and a slab surface temperature exceeding 925 °C, which is a slightly higher temperature than recent estimates from thermal models for the Banda arc.

This recycling of 'crustal', non-radiogenic Hf isotope signatures strongly affects the Hf isotope signatures of newly formed crust at convergent plate settings. The inherited crustal signature results in artificially old crust-formation model ages of new, juvenile crust, similar to the effect of mixing suggested for Nd model ages (Arndt and Goldstein, 1987). This is also true for rocks and associated zircons with $\delta^{18}O < 6.5$. Hence, interpretations based on Hf model ages of such rocks need careful evaluation.

Elevated $\delta^{18}O$ values (i.e., between 6‰ and 8‰) accompanied by low Hf isotope compositions (as compared to the mantle) are recorded for zircons from the Hadaean or early Archaean eons. Our data suggest that subduction zones, including the return of subducted Hf consequent to sediment recycling, are possible geotectonic settings for the formation of some of these zircons. This is supported by the fact that Hadaean or early Archaean eons are more susceptible to melting of SCM than present-day environments due to higher geotherms in the early Earth.

Acknowledgements

This study benefited from stimulating discussions with Yona Nebel-Jacobsen, Daniela Rubatto, Jörg Herman, Hugh O'Neill, Catherine Chauvel, Robert Rapp and Jon Blundy. Bas van der Wagt and Richard Smeets are kindly thanked for laboratory assistance. This work was funded by a NWO (Netherlands Organisation for Scientific Research) grant to PZV (grant no. 814.01.007). The MC-ICPMS facility at VU University Amsterdam is supported by NWO grant no. 175.107.404.01. We thank journal editor Mark Harrison, and Jon Patchett and one anonymous reviewer for thoughtful, constructive and detailed comments.

References

Adam, J., Green, T., 2006. Trace element partitioning between mica- and amphibole-bearing garnet lherzolite and hydrous basanitic melt: 1. Experimental results and the investigation of controls on partitioning behaviour. Contrib. Mineralog. Petrol. 152, 1–17.

Arculus, R.J., Powell, R., 1986. Source component mixing in the regions of arc magma generation. J. Geophys. Res. 91, 5913–5926.

Arndt, N., Goldstein, S., 1987. Use and abuse of crust-formation ages. Geology 15, 893–895.

Barry, T.L., Pearce, J.A., Leat, P.T., Millar, I.L., Le Roex, A.P., 2006. Hf isotope evidence for selective mobility of high-field-strength elements in a subduction setting: South Sandwich Islands. Earth Planet. Sci. Lett. 252, 223–244.

Blichert-Toft, J., Albarede, F., 2008. Hafnium isotopes in Jack Hills zircons and the formation of the Hadean crust. Earth Planet. Sci. Lett. 265, 686–702.

Blichert-Toft, J., Chauvel, C., Albarède, F., 1997. Separation of Hf and Lu for high-precision isotope analysis of rock samples by magnetic sector-multiple collector ICP-MS. Contrib. Mineralog. Petrol. 127, 248–260.

Bouvier, A., Vervoort, J.D., Patchett, P.J., 2008. The Lu–Hf and Sm–Nd isotopic composition of CHUR: constraints from unequilibrated chondrites and implications for the bulk composition of terrestrial planets. Earth Planet. Sci. Lett. 273, 48–57.

Bowin, C., Purdy, G.M., Johnston, C., Shor, G., Lawver, L., Hartono, H.M.S., Jezek, P., 1980. Arc-continant collision in Banda Sea region. Bull. AAPG 64, 868–915.

Brenan, J.M., Shaw, H.F., Ryerson, F.J., Phinney, D.L., 1995. Mineral-aqueous fluid partitioning of trace-elements at 900 °C and 2.0 GPa — constraints on the trace element chemistry of mantle and deep crustal fluids. Geochim. Cosmochim. Acta 59, 3331–3350.

Carpentier, M., Chauvel, C., Maury, R.C., Mattielli, N., 2009. The 'zircon effect' as recorded by the chemical and Hf isotope compositions of Lesser Antilles forearc sediments. Earth Planet. Sci. Lett. 287, 86–99.

Cavosie, A.J., Kita, N.T., Valley, J.W., 2009. Primitive oxygen-isotope ratio recorded in magmatic zircon from the Mid-Atlantic Ridge. Am. Mineralog. 94, 926–934.

Cavosie, A.J., Valley, J.W., Wilde, S.A., 2005. Magmatic delta O-18 in 4400–3900 Ma detrital zircons: a record of the alteration and recycling of crust in the Early Archean. Earth Planet. Sci. Lett. 235, 663–681.

Chauvel, C., Blichert-Toft, J., 2001. A hafnium isotope and trace element perspective on melting of the depleted mantle. Earth Planet. Sci. Lett. 190, 137–151.

Chauvel, C., Lewin, E., Carpentier, M., Arndt, N.T., Marini, J.C., 2008. Role of recycled oceanic basalt and sediment in generating the Hf–Nd mantle array. Nat. Geosci. 1, 64–67.

Chauvel, C., Marini, J.C., Plank, T., Ludden, J.N., 2009. Hf–Nd input flux in the Izu–Mariana subduction zone and recycling of subducted material in the mantle. Geochem. Geophys. Geosyst. 10.

Claiborne, L.L., Miller, C.F., Walker, B.A., Wooden, J.L., Mazdab, F.K., Bea, F., 2006. Tracking magmatic processes through Zr/Hf ratios in rocks and Hf and Ti zoning in zircons: an example from the Spirit Mountain batholith. Nev. Mineralog. Mag. 70, 517–543.

Class, C., Miller, C.F., Goldstein, S.L., Langmuir, C.H., 1999. Distinguishing melt and fluid subduction components in Umnak Volcanics, Aleutian Arc. Geochem. Geophys. Geosyst. 1.

Eiler, J.M., Crawford, A., Elliott, T., Farley, K.A., Valley, J.W., Stolper, E.M., 2000. Oxygen isotope geochemistry of oceanic-arc lavas. J. Petrol. 41, 229–256.

Elburg, M.A., Foden, J.D., van Bergen, M.J., Zulkarnain, I., 2005. Australia and Indonesia in collision: geochemical sources of magmatism. J. Volcanol. Geoth. Res. 140, 25–47.

Elburg, M.A., van Bergen, M.J., Foden, J.D., 2004. Subducted upper and lower continental crust contributes to magmatism in the collision sector of the Sunda–Banda arc, Indonesia. Geology 32, 41–44.

Fichtner, A., de Witt, M., van Bergen, M., 2010. Subduction of continental lithosphere in the Banda Sea region: combining evidence from full waveform tomography and isotope ratios. Earth Planet. Sci. Lett. 297, 405–412.

Foley, S.F., Barth, M.G., Jenner, G.A., 2000. Rutile/melt partition coefficients for trace elements and an assessment of the influence of rutile on the trace element characteristics of subduction zone magmas. Geochim. Cosmochim. Acta 64, 933–938.

Foley, S.F., 2008. Trace element constraints on Archean magmatic and metamorphic processes. In: Condie, K.C., Pease, V. (Eds.), When Did Plate Tectonics Begin on Planet Earth. Geological Society of Americal special paper.

Hall, R., 2002. Cenozoic geological and plate tectonic evolution of SE Asia and the SW Pacific: computer-based reconstructions, model and animations. J. Asian Earth Sci. 20, 353–431.

Hamilton, W., 1979. Tectonics of the Indonesian region *US GS Prof. papers*. United States Geological Survey.

Harrison, T.M., 2009. The Hadean Crust: Evidence from >4 Ga Zircons. Annu. Rev. Earth Planet. Sci. 37, 479–505.

Harrison, T.M., Blichert-Toft, J., Muller, W., Albarede, F., Holden, P., Mojzsis, S.J., 2005. Heterogeneous Hadean hafnium: evidence of continental crust at 4.4 to 4.5 Ga. Science 310, 1947–1950.

Harrison, T.M., Schmitt, A.K., McCulloch, M.T., Lovera, O.M., 2008. Early (>= 4.5 Ga) formation of terrestrial crust: Lu–Hf, delta O-18, and Ti thermometry results for Hadean zircons. Earth Planet. Sci. Lett. 268, 476–486.

Hawkesworth, C.J., Gallagher, K., Hergt, J.M., McDermott, F., 1993. Mantle and slab contribution to arc magma. Annu. Rev. Earth Planet. Sci. 21, 175–204.

Hawkesworth, C.J., Kemp, A.I.S., 2006. Using hafnium and oxygen isotopes in zircons to unravel the record of crustal evolution. Chem. Geol. 226, 144–162.

Hawkesworth, C.J., Dhuime, B., Pietranik, A.B., Cawood, P.A., Kemp, A.I.S., Storey, C.D., 2010. The generation and evolution of the continental crust. J. Geol. Soc. Lond. 167, 229–248.

Hermann, J., Rubatto, D., 2009. Accessory phase control on the trace element signature of sediment melts in subduction zones. Chem. Geol. 265, 512–526.

Hilton, D.R., Hoogewerff, J.A., van Bergen, M.J., Hammerschmidt, K., 1992. Mapping magma sources in the East Sunda-Banda arcs, Indonesia — constraints from Helium isotopes. Geochim. Cosmochim. Acta 56, 851–859.

Hinschberger, F., Malod, J.A., Dyment, J., Honthaas, C., Rehault, J.P., Burhanuddin, S., 1999. Magnetic lineations constraints for the back-arc opening of the Late Neogene South Banda Basin (eastern Indonesia)*SEASIA International Conference/4th Sino-French Symposium on Active Subduction and Collision in Southeast Asia*, Montpellier, France.

Honthaas, C., Rehault, J.P., Maury, R.C., Bellon, H., Hemond, C., Malod, J.A., Cornee, J.J., Villeneuve, M., Cotten, J., Burhanuddin, S., Guillou, H., Arnaud, N., 1998. A Neogene back-arc origin for the Banda Sea basins: geochemical and geochronological constraints from the Banda ridges (East Indonesia). Tectonophysics 298, 297–317.

Hoogewerff, J.A., van Bergen, M.J., Vroon, P.Z., Hertogen, J., Wordel, R., Sneyers, A., Nasution, A., Varekamp, J.C., Moens, H.L.E., Mouchel, D., 1997. U-series, Sr–Nd–Pb isotope and trace-element systematics across an active island arc-continent collision zone: implications for element transfer at the slab-wedge interface. Geochim. Cosmochim. Acta 61, 1057–1072.

Hopkins, M., Harrison, T.M., Manning, C.E., 2008. Low heat flow inferred from > 4 Ga zircons suggests Hadean plate boundary interactions. Nature 456, 493–496.

Hopkins, M.D., Harrison, T.M., Manning, C.E., 2010. Constraints on Hadean geodynamics from mineral inclusions in > 4 Ga zircons. Earth Planet. Sci. Lett. 298, 367–376.

Jezek, P.A., Hutchinson, C.S., 1978. Banda arc of eastern Indonesia: petrology and geochemistry of the volcanic rocks. Bull. Volcanol. 41, 586–608.

Johnson, K.T.M., 1998. Experimental determination of partition coefficients for rare earth and high-field-strength elements between clinopyroxene, garnet, and basaltic melt at high pressures. Contrib. Mineralog. Petrol. 133, 60–68.

Johnson, M.C., Plank, T., 1999. Dehydration and melting experiments constrain the fate of subducted sediments. Geochem. Geophys. Geosyst. 1.

Kelemen, P.B., Hanghoy, K., 2003. One view of the geochemistry of subduction-related magmatic arcs, with an emphasis on primitive andesite and lower crust. Treatise Geochemstry 3 (18), 593–659.

Kemp, A.I.S., Hawkesworth, C.J., Foster, G.L., Paterson, B.A., Woodhead, J.D., Hergt, J.M., Gray, C.M., Whitehouse, M.J., 2007. Magmatic and crustal differentiation history of granitic rocks from Hf–O isotopes in zircon. Science 315, 980–983.

Kemp, A.I.S., Hawkesworth, C.J., Paterson, B.A., Kinny, P.D., 2006. Episodic growth of the Gondwana supercontinent from hafnium and oxygen isotopes in zircon. Nature 439, 580–583.

Kemp, A.I.S., Wilde, S.A., Hawkesworth, C., Coath, C.D., Nemchin, A., Pidgeon, R.T., Vervoort, J.D., DuFrane, S.A., 2010. Hadean crustal evolution revisited: new constraints from Pb–Hf isotope systematics of the Jack Hills zircons. Earth Planet. Sci. Lett. 296, 45–56.

Kempton, P.D., Pearce, J.A., Barry, T.L., Fitton, J.G., Langmuir, C., Christie, D.M., 2002. Sr–Nd–Pb–Hf isotope results from ODP leg 187: evidence for mantle dynamics of the Australian–Antarctic Discordance and origin of the Indian MORB source. Geochem. Geophys. Geosyst. 3.

Kessel, R., Schmidt, M.W., Ulmer, P., Pettke, T., 2005. Trace element signature of subduction-zone fluids, melts and supercritical liquids at 120–180 km depth. Nature 437, 724–727.

Klimm, K., Blundy, J.D., Green, T.H., 2008. Trace element partitioning and accessory phase saturation during H2O-saturated melting of basalt with implications for subduction zone chemical fluxes. J. Petrol. 49, 523–553.

König, S., Münker, C., Schuth, S., and Garbe-Schönberg, D., 2008. Mobility of tungsten in subduction zones. Earth Planet. Sci. Lett. 274, 82–92.

Lee, C.S., McCabe, R., 1986. The Banda Celebes Sulu basin — a trapped piece of Cretaceous Eocene oceanic crust. Nature 322, 51–54.

Magaritz, M., Whitford, D.J., James, D.E., 1978. Oxygen isotopes and the origin of high $^{87}Sr/^{86}Sr$ anesites. Earth Planet. Sci. Lett. 40, 220–230.

Marini, J.C., Chauvel, C., Maury, R.C., 2005. Hf isotope compositions of northern Luzon arc lavas suggest involvement of pelagic sediments in their source. Contrib. Mineralog. Petrol. 149, 216–232.

McCaffrey, R., 1989. Teleseismic investigation of the January 22, 188 Tennant Creek, Australia, Earthquakes. Geophys. Res. Lett. 16, 413–416.

McCulloch, M.T., Gamble, J.A., 1991. Geochemical and geodynamical constraints on subduction zone magmatism. Earth Planet. Sci. Lett. 102, 358–374.

Menneken, M., Nemchin, A.A., Geisler, T., Pidgeon, R.T., Wilde, S.A., 2007. Hadean diamonds in zircon from Jack Hills, Western Australia. Nature 448, 917-U5.

Mojzsis, S.J., Harrison, T.M., Pidgeon, R.T., 2001. Oxygen-isotope evidence from ancient zircons for liquid water at the Earth's surface 4300 Myr ago. Nature 409, 178–181.

Morel, M.L.A., Nebel, O., Nebel-Jacobsen, Y.J., Miller, J.S., Vroon, P.Z., 2008. Hafnium isotope characterization of the GJ-1 zircon reference material by solution and laser-ablation MC-ICPMS. Chem. Geol. 255, 231–235.

Morris, J.D., Gill, J.B., Schwartz, D., Silver, E.A., 1984. Late Miocene to recent Banda sea volcanism, III: Isotopic compositions EOS.

Münker, C., Pfänder, J.A., Weyer, S., Büchl, A., Kleine, T., Mezger, K., 2003. Evolution of planetary cores and the earth–moon system from Nb/Ta systematics. Science 301, 84–87.

Münker, C., Weyer, S., Scherer, E., Mezger, K., 2001. Separation of high field strength elements (Nb, Ta, Zr, Hf) and Lu from rock samples for MC-ICPMS measurements. Geochem. Geophys. Geosyst. 2.

Münker, C., Wörner, G., Yogodzinski, G.M., Churikova, T.G., 2004. Behaviour of high field strength elements in subduction zones: constraints from Kamtchatka–Aleutian arc lavas. Earth Planet. Sci. Lett. 224, 275–293.

Nebel-Jacobsen, Y.J., Münker, C., Nebel, O., Gerdes, A., Mezger, K., Nelson, D.R., 2010. Reworking of Earth's first crust: constraints from Hf isotopes in Archean zircons from Mt. Narryer. Aust. Precambrian Res. 182, 175–186.

Nebel, O., Morel, M.L.A., Vroon, P.Z., 2009. Isotope dilution analyses of Lu, Hf, Zr, Ta and W, and Hf-isotope compositions of NIST SRM-610 and SRM-612 glass wafers. Geostand. Geoanal. Res. 33.

Nebel, O., Münker, C., Nebel-Jacobsen, Y.J., Kleine, T., Mezger, K., Mortimer, N., 2007. Hf–Nd–Pb isotope evidence from Permian arc rocks for the long-term presence of the Indian-Pacific mantle boundary in the SW Pacific. Earth Planet. Sci. Lett. 254, 377–392.

Nebel, O., van Westrenen, W., Vroon, P.Z., WIlle, M., Raith, M.M., 2010a. Deep mantle storage of the Earth's missing niobium in late-stage residual melts from a Hadean magma ocean. Geochim. Cosmochim. Acta 74, 4392–4404.

Nebel, O., Vroon, P.Z., Wiggers de Vries, D.F., Jenner, F., Mavrogenes, J.A., 2010b. Tungsten isotopes as tracers of core–mantle interactions: the influence of subducted sediments. Geochim. Cosmochim. Acta 74, 751–762.

Nemchin, A., Whitehouse, M., Pidgeon, R.T., Meyer, C., 2006. Oxygen isotopic signature of 4.4–3.9 Ga zircons as a monitor of differentiation processes on the Moon. Geochim. Cosmochim. Acta 70, 1864–1872.

Nowell, G.M., Kempton, P.D., Noble, S.R., Fitton, J.G., Saunders, A.D., Mahoney, J.J., Taylor, R.N., 1998. High precision Hf isotope measurements of MORB and OIB by thermal ionisation mass spectrometry; insights into the depleted mantle. Chem. Geol. 149, 211–233.

Patchett, P.J., Kouvo, O., Hedge, C.E., Tatsumoto, M., 1981. Evolution of continental crust and mantle heterogeneity: evidence from Hf isotopes. Contrib. Mineralog. Petrol. 78, 279–297.

Patchett, P.J., Vervoort, J.D., Söderlund, U., Salters, V.J.M., 2004. Lu–Hf and Sm–Nd isotopic systematics in chondrites and their constraints on the Lu–Hf properties of the Earth. Earth Planet. Sci. Lett. 222, 29–41.

Pearce, J.A., Kempton, P.D., Gill, J.B., 2007. Hf–Nd evidence for the origin and distribution of mantle domains in the SW Pacific. Earth Planet. Sci. Lett. 260, 98–114.

Pearce, J.A., Kempton, P.D., Nowell, G.M., Noble, S.R., 1999. Hf–Nd element isotope perspective on the nature and provenance of mantle and subduction components in Western Pacific arc-basin systems. J. Petrol. 40, 1579–1611.

Peck, W.H., Valley, J.W., Wilde, S.A., Graham, C.M., 2001. Oxygen isotope ratios and rare earth elements in 3.3 to 4.4 Ga zircons: ion microprobe evidence for high delta O-18 continental crust and oceans in the Early Archean. Geochim. Cosmochim. Acta 65, 4215–4229.

Pietranik, A.B., Hawkesworth, C.J., Storey, C.D., Kemp, A.I.S., Sircombe, K.N., Whitehouse, M.J., Bleeker, W., 2008. Episodic, mafic crust formation from 4.5 to 2.8 Ga: new evidence from detrital zircons, Slave craton, Canada. Geology 36, 875–878.

Plank, T., Cooper, L.B., Manning, C.E., 2009. Emerging geothermometers for estimating slab surface temperatures. Nat. Geosci. 2, 611–615.

Rubatto, D., Hermann, J., 2007. Experimental zircon/melt and zircon/garent trace element partitioning and implications for the geochronology of crustal rocks. Chem. Geol. 241, 38–61.

Rudnick, R.L., Gao, S., 2003. The composition of the continental crust. Treatise Geochemstry 3.

Salters, V.J.M., Hart, S.R., 1991. The mantle sources of ocean ridges, islands and arcs — the Hf isotope connection. Earth Planet. Sci. Lett. 104, 364–380.

Salters, V.J.M., Stracke, A., 2004. Composition of the depleted mantle. Geochem. Geophys. Geosyst. 5.

Salters, V.J.M., White, W.M., 2004. Hf isotope constraints on mantle evolution. Chem. Geol. 145, 447–760.

Stolz, A.J., Varne, R., Davies, G.R., Wheller, G.E., Foden, J.D., 1990. Magma source components in an arc–continent collision zone — the Flore–Lembata sector, Sunda arc, Indonesia. Contrib. Mineralog. Petrol. 105, 585–601.

Syracuse, E.M., van Keken, P.E., Abers, G.A., 2010. The global range of subduction zone thermal models. Phys. Earth Planet. Inter. 183, 73–90.

Taylor, D.J., McKeegan, K.D., Harrison, T.M., 2009. Lu–Hf zircon evidence for rapid lunar differentiation. Earth Planet. Sci. Lett. 279, 157–164.

Thirlwall, M.F., Graham, A.M., Arculus, R.J., Harmon, R.S., Macpherson, C.G., 1996. Resolution of the effects of crustal assimilation, sediment subduction, and fluid transport in island arc magmas: Pb–Sr–Nd–O isotope geochemistry of Grenada, Lesser Antilles. Geochim. Cosmochim. Acta 60, 4785–4810.

Todd, E., Gill, J.B., Wysoczanski, R.J., Handler, M.R., Wright, I.C., Gamble, J.A., 2010. Sources of constructional cross-chain volcanism in the southern Havre Trough: new insights from HFSE and REE concentration and isotope systematics. Geochem. Geophys. Geosyst. 11.

Tollstrup, D.L., Gill, J.B., 2005. Hafnium systematics of the Mariana arc: evidence for sediment melt and residual phases. Geology 33, 737–740.

Tollstrup, D.L., Gill, J.B., Prinkey, D., Williams, R., Tamura, Y., Ishizuka, O., 2010. Across-arc geochemical trends in the Izu Bonin arc: contributions from the subducted slab, revisited. Geochem. Geophys. Geosyst. 11.

Trail, D., Mojzsis, S.J., Harrison, T.M., Schmitt, A.K., Watson, E.B., Young, E.D., 2007. Constraints on Hadean zircon protoliths from oxygen isotopes, Ti-thermometry, and rare earth elements. Geochem. Geophys. Geosyst. 8.

Turner, S., Handler, M., Bindeman, I., Suzuki, K., 2009. New insights into the origin of O–Hf–Os isotope signatures in arc lavas from Tonga-Kermadec. Chem. Geol. 266, 196–202.

Ushikubo, T., Kita, N.T., Cavosie, A.J., Wilde, S.A., Rudnick, R.L., Valley, J.W., 2008. Lithium in Jack Hills zircons: evidence for extensive weathering of Earth's earliest crust. Earth Planet. Sci. Lett. 272, 666–676.

Valley, J.W., Lackey, J.S., Cavosie, A.J., Clechenko, C.C., Spicuzza, M.J., Basei, M.A.S., Bindeman, I.N., Ferreira, V.P., Sial, A.N., King, E.M., Peck, W.H., Sinha, A.K., Wei, C.S., 2005. 4.4 billion years of crustal maturation: oxygen isotope ratios of magmatic zircon. Contrib. Mineralog. Petrol. 150, 561–580.

Valley, J.W., Peck, W.H., King, E.M., Wilde, S.A., 2002. A cool early Earth. Geology 30, 351–354.

van Bergen, M.J., Vroon, P.Z., Hoogewerff, J.A., 1993. Geochemical and tectonic relationships in the East Indonesian arc-continent collision region: implications for the subduction of the Australian passive margin. Tectonophysics 223, 97–116.

van Westrenen, W., Blundy, J.D., Wood, B.J., 2001. High field strength element/rare earth element fractionation during partial melting in the presence of garnet: implications for identification of mantle heterogeneities. Geochem. Geophys. Geosyst. 2 Paper number 2000GC000133.
Vervoort, J.D., Blichert-Toft, J., 1999. Evolution of the depleted mantle: Hf isotope evidence from juvenile rocks through time. Geochim. Cosmochim. Acta 63, 533–556.
Vervoort, J.D., Patchett, P.J., 1996. Behavior of hafnium and neodymium isotopes in the crust: constraints from Precambrian crustally derived granites. Geochim. Cosmochim. Acta 60, 3717–3733.
Vervoort, J.D., Patchett, P.J., Blichert-Toft, J., Albarede, F., 1999. Relationships between Lu–Hf and Sm–Nd isotopic systems in the global sedimentary system. Earth Planet. Sci. Lett. 168, 79–99.
Vroon, P.Z., Lowry, D., van Bergen, M.J., Boyce, A.J., Mattey, D.P., 2001. Oxygen isotope systematics of the Banda Arc: low delta O-18 despite involvement of subducted continental material in magma genesis. Geochim. Cosmochim. Acta 65, 589–609.
Vroon, P.Z., van Bergen, M.J., Klaver, G.J., White, W.M., 1995. Strontium, neodymium, and lead isotopic and trace-element signatures of the east Indonesian sediments — provenance and implications for Banda arc magma genesis. Geochim. Cosmochim. Acta 59, 2573–2598.
Vroon, P.Z., van Bergen, M.J., White, W.M., Varekamp, J.C., 1993. Sr–Nd–Pb Isotope Systematics of the Banda Arc, Indonesia — combined Subduction and Assimilation of Continental Material. J. Geophys. Res. Solid Earth 98, 22349–22366.
Watson, E.B., Harrison, T.M., 1983. Zircon saturation revisited — temperature and composition effects in a variety of crustal magma types. Earth Planet. Sci. Lett. 64, 295–304.
Weyer, S., Münker, C., Mezger, K., 2003. Nb/Ta, Zr/Hf and REE in the depleted mantle: implications for the differentiation history of the crust–mantle system. Earth Planet. Sci. Lett. 205, 309–324.
White, W.M., Patchett, J., 1984. Hf–Nd–Sr-isotopes and incompatible element abundances in island arcs; implications for magma origins and crust-mantle evolution. Earth Planet. Sci. Lett. 67, 167–185.
Whitford, D.J., Jezek, P.A., 1979a. Origin of late-Cenozoic lavas from the Banda arc, Indonesia — trace element and Sr isotope evidence. Contrib. Mineralog. Petrol. 68, 141–150.
Whitford, D.J., Jezek, P.A., 1979b. Origin of Late-Cenozoic lavas from the Banda arc, Indonesia - trace element and Sr isotope evidence. Contrib. Mineralog. Petrol. 68, 141–150.
Wilde, S.A., Valley, J.W., Peck, W.H., Graham, C.M., 2001. Evidence from detrital zircons for the existence of continental crust and oceans on the Earth 4.4 Gyr ago. Nature 409, 175–178.
Woodhead, J.D., Eggins, S.M., Johnson, R.W., 1998. Magma genesis in the New Britain island arc: further insights into melting and mass transfer process. J. Petrol. 39, 1641–1668.
Woodhead, J.D., Hergt, J.M., Davidson, J.P., Eggins, S.M., 2001. Hafnium isotope evidence for 'conservative' element mobility during subduction zone processes. Earth Planet. Sci. Lett. 192, 331–346.
Yogodzinski, G.M., Vervoort, J.D., Brown, S.T., Gerseny, M., 2010. Subduction controls of Hf and Nd in lavas of the Aleutian island arc. Earth Planet. Sci. Lett. 300, 226–238.